Desalination and Water Treatment
www.deswater.com

doi:10.5004/dwt.2018.23119

135 (2018) 1–15
December

Understanding bioswale as a small water and wastewater treatment plant: A theoretical review

Joshua Lelemia Irvine, Albert S. Kim*

Civil and Environmental Engineering, University of Hawaii, Manoa, 2540 Dole Street Holmes 383, Honolulu, Hawaii 96822, USA, Tel. +1-808-956-9629, Fax +1-808-956-5014, email: joshuair@hawaii.edu (J.L. Irvine), Tel. +1-808-956-3718, Fax +1-808-956-5014, email: albertsk@hawaii.edu *(A.S. Kim)*

Received 15 June 2018; Accepted 12 September 2018

ABSTRACT

Stormwater threats can be mitigated with the application of sustainable and renewable technologies such as low-impact development (LID) and best management practice (BMP). This paper aims to fill the present gap in practical applications and engineering science regarding modeling bioswales, a type of LID/BMP devices. Included is a new theoretical framework that treats bioswales as combined physico-chemical processes. A discussion of a coherent analogy between the bioswale and a conventional water and wastewater treatment plant (WWWTP) is presented without including biological processes. Finally, we provide new perspectives regarding computational fluid dynamics (CFD) for widespread use as a promising tool to optimize LID/BMP design for stormwater management.

Keywords: Bioswale; Computational fluid dynamics; Best management practice; Low-impact development; Design optimization; Stormwater runoff

1. Introduction

Low-impact development (LID) and best management practice (BMP) are important components within the praxis of stormwater management. These management practices have evolved considerably in the last five decades. In 1972, the United States (US) created the National Pollution Discharge Elimination Systems (NPDES) program through the legalization of Section 402 of the federal Clean Water Act. This action further led to the US Congress amending the Water Quality Act in 1987, which established a framework for regulating the quality of stormwater discharges. The NPDES permit, which is issued by the US Environmental Agency (EPA) or an authorized State [1], has been functional since the 1990s. Subsequently, the term BMP entered mainstream usage with the intention to control stormwater quality and treat storm flows within urban areas by emulating pre-development flow regimes [2].

Structural BMPs include the application of artificial units such as infiltration, filtration, detention/retention systems, wetlands, vegetated systems, and water quality treatment systems. Nonstructural BMPs consist of system maintenance, land-use planning, and outreach programs [3]. A bioretention system (represented by a bioswale) has received close attention in the past thirty years, as it can effectively provide in-situ stormwater quality and quantity control. A bioswale comprises small areas excavated and backfilled with a mixture of high-permeability soil and (optional) organic matter. The systems are often covered with native terrestrial vegetation to provide natural landscaping and maximum infiltration.

The creation of a bioswale, first practiced in Prince George's County, Maryland, USA [4], depends on ecological interactions within a natural system for the runoff reduction and pollutant removal. Interactions between human-made bioswales and the natural environment rely on various physico-chemical factors, such as precipitation patterns, solute-soil interactions, and size of sediment particles and soil grains. The infiltration occurs after the runoff process starts until the bioswale is fully saturated, but the transport phenomenon has a wide span of timescales within this context. Stormwater infiltration and pollutant

*Corresponding author.

convection occur within the order of a few hours, which depends on the size and porosity of the bioswale [5]. The evapotranspiration requires a considerably longer time span—an order of a few days—based on the characteristics of the vegetation and topsoil layers [5,6].

Bioswale modeling is critical for optimal designs, cost-effective building, and long-term maintenance. To date, most simulation investigations on bioswales are limited to the analysis of experimental data and modeling macroscale (e.g., watershed) water balances. Specifically, bioswale modeling research related to hydrology and hydrodynamics include runoff and infiltration [7–9], urban water management employing fuzzy logic [10], water reuse [11], runoff volume reduction at a watershed level [12,13], urban runoff control with the System for Urban Stormwater and the Analysis Integration (SUSTAIN) model [14] and DRAINMOD [15]. Palla and Gnecco simulated the hydrologic responses of an urban catchment for various rainfall scenarios using the EPA Storm Water Management Model (SWMM) with LID control modules for a large land area of 5.5 ha [16]. Their results confirmed that land use should be minimized for effective LID operation, and hydrologic performance improves as the size of the effective impervious area decreases. Xu et al. asserted that SWMMM provides the highest level of accuracy in design tools [17]. In particular, Xu et al. investigated optimal ratios of land-use/land-cover for the development of urban catchments, however, this approach did not consider localized phenomena to optimize the performance of a single LID device. Similarly, Bloorchian et al. used the personal computer stormwater management model (PCSWMM) which is a GIS version of EPA SWMM. This method is an idealized subcatchment approach to simulate runoff reduction within a bioswale, vegetated filter strip, and infiltration trench using the Manning's equation [18]. Other modeling studies directly related to bioswale have investigated the removal of suspended solids and metal ions from the urban runoff flows [19–21]. For bioretention systems, Brown et al. predicted the continuous, long-term hydrologic response of the technology to influent runoff using DRAINMOD [15]. The calibrated and validated model predicted runoff volume for contributing area runoff of varying imperviousness. Similarly, Hathaway et al. studied bioretention function under possible climate change scenarios in North Carolina, USA, utilizing calibrated DRAINMOD models to establish hydrologic regimes under present day and projected future climate scenarios [22]. Their study focused primarily on water balances to cope with increased rainfall magnitude instead of dealing with specific chemical, physical, and biological transport phenomena. However, these modeling studies were limited to the analysis of experimentally observed data and did not consider a range variation of bioswale configurations.

Green roof systems, a type of LID device, perform similar primary functions as a bioswale with regards to runoff reduction and pollutant removal. Stovin et al. developed a conceptual hydrological flux model and used 30-year hourly climate projections in multiple United Kingdom locations to simulate the long-term runoff and drought risk associated with the application of green-roof systems [23]. Their modeling methodology was based on solving governing equations of large scales from hydrological and agricultural science literature. A comprehensive review study concerning green roof's hydrologic performance can be found elsewhere in the literature [24]. A similar technique can be employed to estimate a long-term performance of unit bioswale systems based on fundamental governing equations in fluid mechanics. We believe that computational fluid dynamics (CFD) modeling is a more accurate simulation approach, which can also predict the momentum and mass transport across the bioswale. The coupling of surface and porous-media flows with non-volatile solute transport in an aqueous phase, however, presents a difficult task in the achievement of rigorous modeling of bioswale systems. Afrin et al.'s most recent CFD work investigated the flow field through a perforated drainage pipe [25], but their work did not include coupling of the overland and infiltration flows on the top bioswale surface. For accurate prediction and design optimization of bioswales, a holistic modeling framework is of great necessity, which can consist of dominant transport mechanisms and governing equations for each subzone within the bioswale.

This review paper proposes that a bioswale, on a theoretical level, can be considered as a combined unit process of hydraulic, chemical, and biological treatments. Therefore, the paper describes a coherent analogy between the bioswale and a conventional water and wastewater treatment plant (WWWTP). The theoretical framework includes dominant transport mechanisms and governing equations for accurate prediction and design optimization. Finally, our work provides new perspectives of using CFD as a universal modeling platform to specifically investigate coupled transport phenomena in bioswale systems.

2. Theoretical review of basic transport phenomena

This section includes the fundamentals of transport phenomena in direct relation to those that take place in a bioswale. The momentum transfer phenomena include overland surface flow, outgoing overflow, infiltration, and drainage; and the mass transfer phenomena comprises sedimentation, granular media filtration (GMF), and granular activated carbon (GAC) adsorption. Our technical review focuses on specific models of each subprocess with governing equations, which can further enhance a holistic understanding of the bioswale transport phenomena.

2.1. Overview of specific processes

A bioswale contains numerous external and internal components. An inlet structure is created in a bioswale as a slanted surface to direct urban runoff from the surrounding areas. The top area of a bioswale is designed to store ponded water. An overflow bypass diverts accumulated water that exceeds the respective unit's ponding capacity. An underdrain structure, or pipe, can be optionally installed at the bottom of the unit to prevent unnecessary water stagnation over a prolonged period. Filtration media is an amended soil that contains considerably higher permeability compared to those of the natural ambient soil materials. Considering the previously mentioned structural aspects, a bioswale can be perceived to form a miniature WWWTP.

Fig. 1 offers a schematic diagram of a typical bioswale system. In this study, we analyze transport phenomena in a bioswale, considered as a complex system containing numerous unit processes as described as follows. First, the inlet structure and the top surface of a bioswale usually contain vegetation layers, consisting of grasses, low-growing plants and ground cover, which are short plants. These vertically embedded natural objects offer hydraulic resistances to runoff water and capture large debris on or within the vegetation layers. One of the functions of the vegetation layer is analogous to the performance of bar racks in WWWTP. The top surface of a bioswale is often located slightly below the overflow structure in order to generate a necessary ponding capacity. Runoff water flows in a lateral direction from the inlet to the outlet sides. As the vegetation in this potential ponding zone offers significant hydraulic resistance, flow deceleration can enhance the sedimentation rate of large particulate materials on orders of 10 microns or above. Second, a mulch layer may cover the root zone of the plants, which can provide organic environments for small living organisms [26,27]. This mulch layer is installed to conserve soil moisture and prevent weed growth. Conversely, a dry mulch layer absorbs initial rainwater and contributes to the removal of specific chemicals in runoff water. Third, the granular soil media has high permeability and is often mixed with organic matter to enable the adsorptive removal of organic pollutants. The combined media, consisting of the top mulch layer and the internal mixed-soil zone, can play similar roles of GMF of particulate materials, GAC adsorption of organic matter, and biological degradation of inorganic pollutants in the WWWTP.

Fourth, the porous zone covering the underdrain pipe comprises gravel or stones, which possess considerable hydraulic conductivity. This underground drainage mimics the distributing unit of WWWTPs, because discharged water may not contain a higher pollutant concentration than that within the runoff. Primarily, a bioswale can significantly reduce stormwater volumes through real-time infiltration and post-storm evapotranspiration. The bottom drain zone of a bioswale can be specifically designed to retain previously infiltrated water until the occurrence of the next storm event. As the hydraulic permeability of the bioswale soil is usually considerably higher as compared to that of the ambient soil, the permeability at underground boundaries between the bioswale and ambient soil zones may not serve as a significant factor so as to estimate the bioswale performance. Fifth, the water volume, initially reduced by a dry bioswale, is equal to the internal void volume of the bioswale (i.e., the overall volume multiplied by the average porosity of the composting soil media). When a dry bioswale becomes fully saturated with infiltrated water, various pollutants from non-point sources can be captured and removed by the bioswale at the point sink. Prediction of the pollutant removal by the bioswale is a difficult task because the chemical and biological characteristics of the bioswale are only partially known. In this section, we specifically characterize a bioswale in terms of overland and infiltration flows, vegetation layer of high hydraulic resistance, sedimentation of suspended solids in the vegetation layer, GMF of fine particles by soil grains, GAC process for the adsorption of organic matter, and underground drainage. Pollutant removal using microorganisms living in the bioswale is another important topic, which is, however, out of our research scope, as the fluid flow and chemical transport significantly influence biological activities in engineered systems. Conventional and contemporary theories are introduced to investigate the complex transport phenomena in the bioswale.

Overland flow on the bioswale surface consists of inflow and overflow of the bioswale, and the fractional difference between these two flow types is equivalent to the infiltration flow. Darcy's law and the principle of continuity of flow through a porous media dictate the form of equations prescribed to describe the infiltrating motion of water through

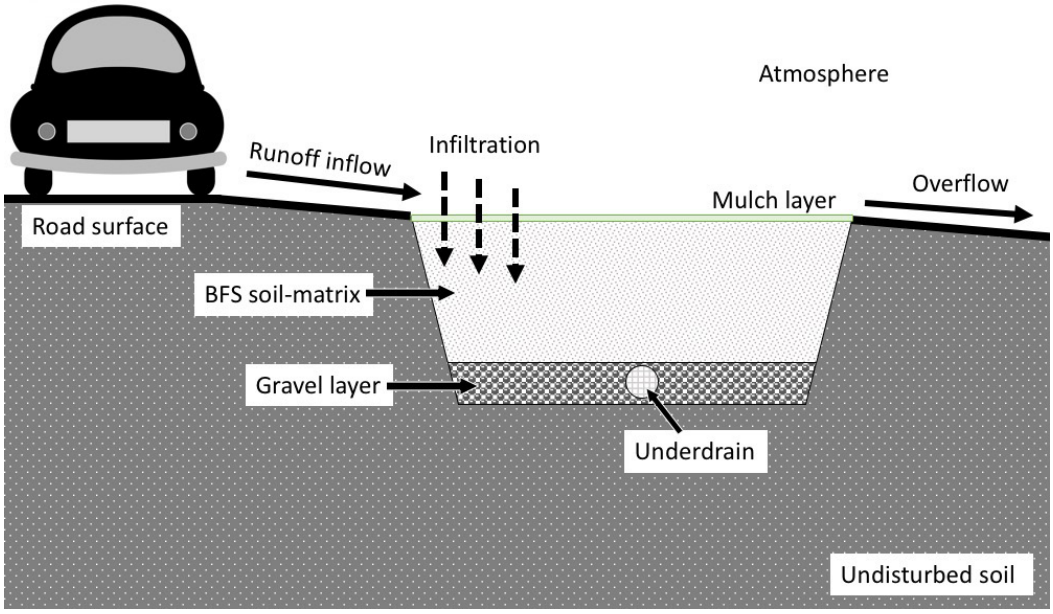

Fig. 1. Schematic of a typical bioswale system.

a particular kind of soil. As water is an incompressible fluid, flow rates of the inflow, overflow, and infiltration flow are strongly coupled by the constant density and viscosity of water. The rigorous numerical solution that completely couples groundwater to surface water through a non-homogeneous soil is represented by the Richards equation.

$$\frac{\partial \theta}{\partial t} = \frac{\partial}{\partial z}\left[K(\theta)\left(\frac{\partial h}{\partial t} + 1 \right) \right] \tag{1}$$

where K represents the hydraulic conductivity, h implies the matrix head induced by capillary action as a function of x and y in three-dimensional space, z refers to the elevation above the vertical datum, θ is the volumetric water content, and t is time. The Richards equation, in reality, comprises of several models and numerical techniques for a better approximation of infiltration, and the multidimensional Richards equation can be applied to simulate the solute transport for various cases but barely used to investigate LID/BMP systems [28].

2.2. Flows in free and porous spaces

If the solid matrix possesses uniform porosity and a constant saturation ratio initially, then some theoretical approximation are available to solve the infiltration flux for a single rainfall event [29–32]. Green and Ampt assumed that the soil surface is covered by a thin water layer with negligible thickness [29], which implies that its infiltration capacity f_p constitutes a linear function of S/L.

$$f_p = K_s\left(S/L + 1 \right) \tag{2}$$

where S represents the capillary suction at the wetting front, L forms the distance from the soil surface to the wetting front, and K_s represents the hydraulic conductivity of a saturated zone. However, Mein and Larson [30] re-defined the infiltration capacity

$$f_p = \frac{dF}{dt} = K_S\left(1 + \frac{S\Delta\theta}{F} \right) \tag{3}$$

where F is the cumulative depth of infiltration, equivalent to $S\Delta\theta$, and $\Delta\theta$ represents the initial moisture deficit. The Green-Ampt Mein-Larson approach presumes the slope of the energy line as identical to the slope of the flow plane. These basic mass balance equations implicitly assume that the overland flow of a finite water-depth does not affect the infiltration rate.

For a shallow overland flow, a kinematic wave equation is expressed as

$$\frac{\partial A}{\partial t} + \frac{\partial Q}{\partial x} = j_e b \tag{4}$$

where A represents the wetted cross-sectional area of the plane flow, Q the discharge rate, j_e the rainfall excess (velocity), and b stands for the lateral extent of the flow. Eq. (4) indicates that the precipitation flow rate equals the difference between the inflow plus the discharge rates per length along the direction of the surface flow. The velocity and pressure gradients, nevertheless, are still assumed to be negligible in this case.

In CFD, a free-surface can be modeled to track and locate the phase interface using the volume of fluid (VOF) method [33,34]. A two-phase flow of incompressible and immiscible fluids of air and water with a specific surface tension can be examined in a full domain consisting of an open space, a porous medium, and their interface. Instead of dealing with transport in each phase separately, a phase-averaging method was employed in the VOF method. For a mixture of water (denoted as 1) and air (denoted as 2) in a fluid cell, their fractions (α) should satisfy the sum rule $\sum_{i=1}^{2}\alpha_i = \alpha_1 + \alpha_2 = 1$, indicating that the volume of the fluids is invariant. The evolution of α_i is governed by the following transport equation:

$$\frac{\partial \alpha_i}{\partial t} + U \cdot \nabla \alpha_i = 0 \tag{5}$$

where U represents the mean velocity of the fluid cell because all the fluid is assumed to be incompressible in the VOF method. The incompressible form of the governing equation includes the zero divergence of U ($\nabla \cdot U = 0$). The Navier-Stokes (N-S) equation for this case is

$$\frac{\partial U}{\partial t} + \nabla \cdot (UU) - \nabla \cdot (\nu \nabla U) = -\nabla p \tag{6}$$

where v represents the kinematic viscosity and p forms the pressure. The basic balance Eqs. (5)–(6) of the VOF method can be employed to accurately simulate the overland flows on various types of porous surfaces. To the best of our knowledge, CFD applications for the initial design stages of bioswales or LID/BMP are limited within the literature.

Fluid dynamic simulations in interstitial spaces between soil grains continue to pose a formidable task for researchers. Instead, the soil media can be treated as a uniform porous media characterized by the use of constant porosity and hydraulic conductivity or permeability. In isotropic porous media, the volumetric flux density q (i.e., the flow rate per unit cross-section) can be expressed using Darcy's law

$$q = \frac{-\kappa}{\mu}\nabla p \tag{7}$$

where κ and μ represent the soil permeability and the water viscosity, respectively. When an inertial effect of the porous media flow is important, the pressure gradient exerts non-linear effectson q, expressed as the Darcy-Forchheimer law

$$\nabla p = \frac{-\mu}{\kappa} q - \frac{\rho}{\kappa_I} |q| q \tag{8}$$

where κ_I represents the inertial permeability. Note that q implies an average flow rate of fluid through a porous media per unit cross section, equal to the incoming or exiting velocity of the porous medium. In this case, we have $q = U$ on the boundary between the free and soil spaces. The microscopic fluid speed between adjacent soil grains must exceed q and be approximately equal to q divided by the average porosity.

In a 2017 study, García-Serrana et al. discussed significant issues on bioswale modeling research [35]. These issues are summarized as follows: (1) seamless integration of the

overland flow and infiltration models, as the overland flow is influenced by slopes and lateral surface properties; (2) the accuracy of the side-slope model, which is currently limited to Manning's equation adopting the slope and roughness parameters; (3) optimal relationship between the lateral slope and surface characteristics of a bioswale; and (4) effects of hydraulic properties on runoff volume reduction. To the best of our knowledge, VOF and Darcy's law, also known as the Darcy-Forchheimer law, have not been combined and applied to investigate the fluid dynamic characteristics of the bioswale at a fundamental level. In our opinion, the theoretical combination constitutes a fundamental approach for the simultaneous modeling of overland and infiltration flows in bioswale. The effect of water depth and speed on the infiltration rate can be systematically examined by considering specific scenarios such as the relative magnitude of rainfall rate, saturated conductivity, and infiltration capacity. The VOF is believed to constitute a reasonably accurate model. This approach can be applied to resolve the runoff flows for impervious rough surfaces. One can examine the optimal conditions for the geometric configuration of the side-slopes and the hydraulic properties of the bioswale soils, which can be employed to optimize the bioswale performance. The bioswale design can be enhanced for specific sites through the consideration of regional patterns of precipitation rates and runoff flows. This fundamental fluid-dynamics approach does not require the calibration of specific parameters utilizing observation or simulation data sets. Bioswale designs will be less sensitive to emperical correlations of transport phenomena, of which universal applications are fundamentally questionable.

2.3. Vegetation layers

The use of asphalt and concrete surfaces has altered environmental hydrodynamics and surface erosion on the natural ground since it was first used to pave streets throughout the US in the 1870s [36]. In practice, the retrofitting of paved surfaces to natural vegetated systems can allow the re-saturation in the first few inches of topsoil, thus reducing stormwater runoff [37,38]. The vegetation layer in a bioswale offers specific hydraulic resistance and modifies the overland flow field [39]. The damping capability of the vegetation layer decelerates the plane flow over the bioswale surface and dissipates the hydrodynamic energy carried by the runoff water. Non-vegetated bioswale surfaces are often subjected to soil erosion, due to low-quality landscaping. The essential plant characteristics for creating a flexible vegetation layer comprise volume-fraction, size, shape, and thickness. Native species plantings are preferred for overall bioswale sustainability, but they do not always provide optimum solutions for hands-free maintenance. The structure of vegetation layers, therefore, require careful design to ensure the optimal, consistent operation of a bioswale. The calculation of the hydraulic resistance of the vegetation layer is a complex task due to the intrinsically flexible features of the plants. Depending on the runoff depth, the vegetation layer can be described as submerged or emergent.

The following review includes further research work on fluid flows over or through rigid and flexible vegetation layers. Vargas-Luna et al. stated that there are limited modeling studies that investigate vegetation effects on morphodynamics, performance, and applicability ranges [40]. In CFD modeling, the vegetation layer can be represented by cylindrical rods if the plants have enough rigidity. Zhang et al. examined the transverse distribution of open-channel velocity through an artificial emergent vegetation layer [41]. Their pairs of large and small buoyant spheres form a chain-like flexible structure, which resembles buoyant-positive emergent plants. They modified Shiono and Knight's work [42] (hereafter referred to as SK) concerning depth-averaged N-S equations and supplemented the vegetation drag force F_d as expressed below:

$$\rho gHS - \frac{1}{8} f U_d^2 + \frac{1}{2}\left(\frac{f}{8}\right)^{1/2} \rho \zeta H^2 \frac{\partial^2 U_d^2}{\partial y^2} - \sum F_d = \frac{\partial\left[H(UV)_d\right]}{\partial y} \quad (9)$$

where ρ represents the fluid (water) density, g constitutes the gravitational acceleration, f the drag coefficient, ζ the transverse eddy viscosity coefficient, H the water depth, S the bed slope, and U and V represent the flow velocity components in x- and y-directions respectively. The subscript d (of U_d and $(UV)_d$) the depth averaging of a respective quantity. A central approximation employed within the Zhang et al.'s approach is $(UV)_d = \overline{k} U_d^2$, where the empirical proportionality $\overline{K}$ is determined by fitting suitable experimental data. An asymptotic solution was developed as follows: $U_d^2 = C_0 + C_1 e^{\beta_1 y} + C_2 e^{\beta_2 y}$, where coefficients C_i and β_i are determined using boundary conditions. Calculated depth-averaged velocities demonstrate reasonable agreement with measured data for various water depths. Differences between measured and simulation results were observed primarily along the interface between the vegetated and non-vegetated domains. This consistent discrepancy must be caused by the strong 3D turbulence flow at the interface. Note that the depth-averaged NS equation is fundamentally limited to the depth of maximum 0.2 m. In a 2013 study, Liu et al. modified the SK method for both emergent and submerged vegetation and derived the depth-averaged velocity and bed shear stress of an open channel flow [43]. Liu et al. discovered that the sign of the secondary flow parameter is determined by the rotational direction of the secondary current cells and is dependent on the flow depth. Thus, it is implied that overlooking secondary flow seems to cause a noticeable computational error.

Since real-world flows are transient, the large-eddy simulation (LES) approach is a standard method for many turbulence investigations. To study the flow, scour, and transport processes, Kim et al. [44] applied the LES approach with a ghost-cell immersed-boundary method proposed by Nabi et al. [45] and computed the flow and bed morphodynamics through model vegetation consisting of emergent rigid cylinders. This approach provided a robust framework of combined hydrodynamic modeling, sediment transport, and a morphodynamic approach. In principle, the LES method resolves the computational issue of the large eddies first and then computes smaller ones with a turbulence closure. The subgrid-scale (SGS) stress deals with the effect of small scales on the resolved turbulence [46]. The morphodynamic model created by Kim et al. mimics the temporal elevation of the bed due to the growth of deposited particles and offers a reasonable agreement between the computation and actual experiments [44]. LES applied with the ghost-cell method, however, does not

accurately account for the fluid velocity of the free surface, which is treated as a rigid surface for local acceleration. Gao et al. employed a 3D LES approach with the finite volume method (FVM) so as to simulate the flow field and buoyant jet dilution through emergent vegetation [47]. The presence of vegetation diminished the channel velocity but promoted strong flow spreading and effluent dilution. Lu and Dai employed various CFD methods (LES, Reynolds-averaged Navier-Stokes, laser Doppler anemometer, and particle image velocimetry) to model 3D flow fields and scalar transport in an open channel consisting of submerged and emergent vegetation layers [48]. Lu and Dai obtained a reasonable agreement between the simulation results and data measurements. In the case of understanding bioswale performance, the LES approach can be applied to simulate flow patterns in the vegetative layer.

Wang et al. examined the interplay between emergent vegetation density and rainfall intensity [49]. They represented the dimensionless drag term, C_d, by modifying the Saint-Vanent equations as a function of bed slope, pressure, advection, and rainfall rate. However, to analyze this correlation, a few parameters should be determined through empirical data fitting. Therefore, the model predictability is limited to available experimental data of a specific bioswale. Bioswale research tends to neglect the heat transfer between runoff water and bioswale soil layers. Larmaei and Mahdi applied the double-decomposed depth-averaged continuity and momentum equations to simulate 2D heat flux, and fluid flows in various vegetation layers [50]. In their work, case studies compared the effects of different plant configurations for emergent and submerged vegetation. It was shown that the vegetation structure primarily influences the flow field followed by the heat flux. For long-term operations, evapotranspiration of the bioswale must depend upon humidity and temperature profiles. This review shows that little research has investigated systematically coupled heat and mass transfer in a bioswale.

Our current understanding of vegetation effects on fluid flow and sediment transport is limited to the use of simple models, which are primarily based on experimental approaches. In the past decade, advances in computational resources have been made to simulate flow fields within vegetation layers, as described previously. However, less explored topics in CFD research include how the vegetation layer controls the particle sedimentation by exerting effective hydrodynamic drag forces and torques. In particular, limited research has been conducted to estimate the apparent coefficient of vegetation drag in terms of plant species, biological characteristics, geometric configurations, and the Reynolds number. Since these flow behaviors in bioswales are very complex, the derivation of analytic solutions through mathematical calculations is a challenging task. Therefore, we suggest CFD simulation as a reliable, complementary tool for the precise prediction of coupled phenomena not only for vegetation fluid dynamics but also for gaining an in-depth understanding of basic transport phenomena of the respective bioswale.

2.4. Sedimentation

Sedimentation plays a significant role in solid-liquid separation. In the initial stages of a precipitation event, stormwater enters the mulch and vegetation layers, where surface clogging occurs initially due to the deposition of organic matter and particulate sediments. Fine particles (less than in diameter) are primarily responsible for surface clogging, which progressively reduces the infiltration rate [51]. A few micron-sized particles are subjected to both the Brownian motion and the shear rate so that the dynamic behavior of the particles is generally hard to predict. The reduced infiltration rate is ascribed to the reduction of soil porosity and, hence, hydraulic conductivity. In practice, it is recommended to replace the bioswale soil mixture every 15 years due to the long-term accumulation of particles and pollutants, which leads to clogging and exhaustion of the bioswale, respectively [52]. Conversely, whether 15 years constitutes a reasonable life expectancy remains contestable. Effective maintenance strategies include the replenishment of the mulch layer, removal of weeds and dead plants, and stabilization of eroded soils [51,52]. Filter strips and grass swales are widely used as a pretreatment for other LID/BMP approaches to prevent premature clogging. When the pollutant removal is less important than the runoff mitigation, swales and filter strips do not contain an engineered filter media or soil matrixes [53–57]. Restoring the bioswale capacity after each storm event must be a more significant issue in the maintenance strategy instead of replacing the engineered soil matrix periodically.

Lu and Dai specifically investigated scalar transport in a flow through a vegetated channel by combining momentum and diffusion equations [48]. Incompressible continuity and N-S equations were employed to attain the momentum transfer. The convection-diffusion-reaction equation was applied for the solute transport in the following manner:

$$\frac{\partial C}{\partial t} + \nabla \cdot (uC) = \nabla \cdot (D_t \nabla C) + S_c \tag{10}$$

where C and D_t are the concentration and effective diffusivity of particles, and S_C represent a source term. Furthermore, the random walk equation was employed to track the diffusing particles, originally studied by [58] as depicted below:

$$x_p(t+\delta t) = x_p(t) + \left(\bar{u}_p + \frac{\partial D_t}{\partial x}\right)\delta t + \xi_p\sqrt{2D_t\delta t} \tag{11}$$

where x_p and $\bar{u}_p$ represent the position and mean velocity of a particle, and ξ_p represents a random number following the normal distribution of zero mean and unit variance. The last term in Eq. (11) represents the Wiener process that considers the average length of the random displacement as proportional to $\sqrt{\delta t}$. Note that, in Eq. (11), the convective displacement increases linearly with δt. Furthermore, the diffusivity D_t superimposes molecular, turbulent, and mechanical diffusivities. The simulation results of this study are consistent with experimental observations, but mass diffusion phenomena appear to be double-counted in Eulerian Eq. (10) and Lagrangian Eq. (11).

Bergman et al. applied a mass balance to model clogging in an infiltration trench (for a single trench) [59]. The performance of two stormwater events was compared using the operation data of the initial three years and periods between years 12–15. They simulated the clogging phenomena and applied Warnaars et al.'s semi-conceptual infiltration model

to verify their predictions [60]. Further, Mikkelsen et al. [61] introduced the clogging trend of a trench and described infiltration rate, Q_f as follows

$$Q_f = K_{fs,bottom} \cdot l \cdot w + K_{fs,sides} \cdot 2h \cdot (l + w) \quad (12)$$

where K_{fs} comprises the field-saturated hydraulic conductivity, estimated using simple flow theory, and l, w, and h represent the trench dimensions. The formation of a clogging layer of fine particles between the soil and trench was modeled with the assumption that the clogging layer thickness increases linearly with respect to time. An effective value of $K_{fs,bottom}$ was formulated as a function of time:

$$K_{effective,bottom}(t) = \frac{b_{tot}}{\sum_{i=1}^{N} \frac{b_i}{K_i}} \approx \frac{b_1}{\frac{b_1}{K_1} + \frac{b_2(t)}{K_2}} = \frac{b_1}{\frac{b_1}{K_1} + \frac{a \cdot t}{K_2}} = \frac{1}{\frac{1}{K_1} + c * t} \quad (13)$$

where the parameter b_i denotes layer thickness, and indexes 1 and 2 denote the initial soil layer below the trench (thickness unknown) and the clogging layer respectively. For simplicity, the soil-layer thickness was assumed to be equivalent to the total thickness of sedimentation. The parameter c varies with the soil layer thickness (b_1), growth rate of the clogging layer (a), and its hydraulic conductivity (K_2). Bergman et al. observed that clogging in the infiltration trench reduced infiltration rates by a factor of 2–4 after the 15th year of operation.

Achleitner et al. used a mass balance to describe the contaminant removal capacity of local infiltration devices, installed within six parking lots [52]. The motivation behind this study revolved around questions regarding whether this considered life expectancy value was feasible. The majority of Cu concentrations were found to be retained in the first 30 *cm* of soil, which did not exceed the limit of 100 mg/kg. This assessment was conducted using mass balance equations for the total accumulation of Cu after 15 years. Only one site out of six was found to exceed the regulatory limit values.

Furthermore, Le Coustumer et al. examined the clogging phenomena of stormwater biofilters in temperate climates, using the results of a long-term (72 weeks) laboratory experiment [62]. They observed that smaller systems, in relation to their catchment loads, demonstrate greater susceptibility to clogging as the hydraulic and sediment loading increases. Specifically, they reported that infiltration systems clog over the 72-week testing period by a decreasing factor of 3.6. In biofilters design, the careful selection of appropriate vegetation and structural sizing is recommended to maintain low clogging phases. The particle deposition layer, however, can serve as a dynamic pretreatment step for long-term media filtration.

In the design of permeable pavements, a clogging factor is computed [63] as follows:

$$Clogging\ Factor = Y_{clog} \cdot Pa \cdot CR \cdot (1 + VR) \cdot \frac{(1 - ISF)}{T \cdot VR} \quad (14)$$

where Y_{clog} constitutes the estimated number of years required for a complete clogging, Pa represents the annual rainfall amount over the site, CR denotes the pavement's capture ratio (defined as the area that contributes runoff to the paved area), VR represents the system's void ratio, ISF constitutes the impervious surface fraction, and T stands for the thickness of pavement layer.

In a 2014 study, Kachchu Mohamed et al. investigated the utility of swales as a pre-treatment for clogging before stormwater enters the permeable pavement systems [64]. They observed that short swales shorter than 10 *m* achieved 50–75% removal of total suspended solids (TSS) and swales longer than 10 *m* only provided a marginal 20% reduction in TSS. Their study does not provide an analytical formulation (validated by experimental observations) to predict optimal swale length depending on various overland flow velocities. These results, however, suggest that excessively long swales may not present a cost-effective solution to treat stormwater runoff.

Sun and Davis investigated the fate of heavy metals (Zn, Cu, Pb, and, Cd) with two mass loadings in laboratory pots for modeling bioretention systems [65]. The treatment of stormwater runoff showed that the removal ratio of the influent metals is higher than 90% within 25 *cm* of the bioretention depth. The removal efficiencies for Zn, Cu, Pb, and Cd are proportional to the contaminant loadings. Based on the laboratory study, soil replacement took place within a depth of 25 *cm*, but the roles of mulch and vegetation layers were not specifically studied.

The current understanding of clogging phenomena was limited to the physical modeling studies used for permeable pavements [66], river morphology [67], and riverbank filtration [68]. Locatelli et al., for example, overlooked clogging in the determination of the static performance parameters of inflow and outflow rates for infiltration trenches, despite the existence of extensive experimental research showing that the build-up increases over runoff time [69]. Thus, additional research is required so as to model clogging reduction when LID/BMP takes place in a treatment train in series. Existing literature does not include a universal modeling technique for LID/BMP systems and specifically does not distinguish between surface and subsurface clogging mechanisms. To the best of our knowledge, there are no studies that have investigated the effects on surface clogging of bioswales from wind erosion and dust particles. We believe that multi-phase and multi-scale CFD may provide a fundamental framework for elucidating the surface and subsurface clogging near top bioswale surfaces.

2.5. Granular media filtration

The basic model for the granular media filtration was first developed by Yao et al. [70]. Without the inclusion of chemical or biological reactions of particles, a filter equation was derived as

$$\ln \frac{C}{C_0} = \frac{-3(1 - \epsilon)\eta\alpha L}{2d_c} \quad (15)$$

where C_0 and C represent influent and effluent concentrations of suspended particles, respectively, ϵ and L form the porosity and length (or depth) of the filter media, respectively, d_c represents the filter grain diameter, and η and α constitute the transport and attachment efficiencies, respectively. The transport efficiency η includes three representative mechanisms: the interception (η_I) of particles moving along streamlines, sedimentation (η_G) of particles due to

gravitational forces, and Brownian diffusion (η_D) based on random displacements. A superposition approach, i.e., $\eta = \eta_I + \eta_G + \eta_D$, is widely applied to combine the three major transport mechanisms [71–73]. To accommodate the effect of dense granular packing, Nelson and Ginn employed Happel's sphere-in-cell porous media model to calculate the effective flow field near grains and capturing efficiency [73]. Various applications of Happel's cell [74] model can be found elsewhere [75–80]. In addition to these basic filtration mechanisms, gradual changes in infiltration capacity based on filter ripening and surface clogging form important practical concerns for long-term stable operation and maintenance of GMF.

The soil matrix of a bioswale is similar to the GMF used in WWWTP, in which suspended solids are removed by the passage of water through a porous media. Unlike that in WWWTP, intermittent wet and dry periods represent unique natural occurrences in the bioswales and, in general, stormwater treatment systems. These conditions may affect the removal of pollutants. The direct application of the GMF theory within a bioswale system requires a restriction that the interstitial spaces between soil grains are completely saturated. A further fundamental investigation is specifically required for particle filtration within the saturating bioswale during coupled runoff-generated infiltration [81–84].

The gain and loss of transported particles on a porous surface are controlled by wind-influenced evapotranspiration intensity in dry weather and rainfall intensity in wet weather [21]. During a storm period, the suspended particles in the runoff stream accumulate upon the bioswale surface and reach a steady state that balances sedimentation, filtration, and overland flow. Delleur reviewed fundamental approaches regarding sewer sediment movement in 2D, which includes roles of bedload movement, suspended load, total load, near-bed solids for both steady and unsteady flows; and emphasized the significance of the particle size distribution [85]. As of 2018, models that can provide analytic equations for the particle transport in unsaturated media are still in a developing stage given current literature and have not been used for bioswale applications.

2.6. Organic and inorganic pollutant removal

Organic materials can be mixed with engineered soil grains to enhance the removal of organic pollutants in runoff water. In the granular activated carbon (GAC) process of WWTPs, an adsorption isotherm quantifies the affinity of the adsorbate (i.e., organic pollutant) for an adsorbent (i.e., GAC). The isotherm is used to describe the ratio of the adsorbate amount adsorbed onto an adsorbent surface at equilibrium condition. If the aqueous-phase concentration of the adsorbate is in a steady state, the adsorption equilibrium capacity can be estimated using the following mass balance

$$q_e = \frac{C_0 - C_e}{M/V} \tag{16}$$

where q_e represents the equilibrium adsorbent-phase concentration of adsorbate [mg-adsorbate/ g-adsorbent], C_0 and C_e represent the adsorbate concentrations in the initial and equilibrium phase, respectively, while M/V indicates the adsorbent mass M per unit volume V. Typically, three types of isotherms are widely used: linear, Langmuir [86], and Freundlich [87]. The Langmuir isotherm assumes a reversible adsorption of an adsorbate, forming a monolayer upon adsorbent surfaces in equilibrium. Then, the rates of adsorption and desorption are assumed to be equal. In the isotherm, a mass loading q_e is derived as:

$$q_e = Q_{\max}\frac{bC_e}{1+bC_e} \; or \; \frac{Q_e}{q_e} = 1 + \frac{1}{bC_e} \tag{17}$$

where b represents the Langmuir adsorption constant of adsorbate and Q_{max} is the maximum limit of q_e. Next, the Freundlich isotherm was originally proposed as an empirical equation to fit non-linear trends of q_e with respect to the equilibrium concentration C_e, which is due to the heterogeneity of adsorbent surfaces:

$$q_a = K_a C_a^{1/n} \; or \; \ln q_a = \ln K_a + \frac{1}{n}\ln C_a \tag{18}$$

where K_a is the adsorption capacity parameter, n is the dimensionless adsorption intensity parameter. In this isotherm, a unit of K_a depends on the value of n. Finally, the linear isotherm represents a special case of Langmuir and Freundlich isotherms known to be valid in solutions of low adsorbate concentrations.

For adsorption of a single component adsorbate, the constant influent concentration, C_{inf} in the mass balance along the depth z is given by

$$\frac{C(z)}{C_{\inf}} = \frac{q(z)}{q_e(C_{\inf})} \tag{19}$$

where $C(z)$ and $q(z)$ are the adsorbate concentrations in the liquid and the adsorbent phases, respectively, at depth z (within the mass transfer zone), and $q_e(C_{inf})$ denotes the adsorbate concentration in equilibrium with the influent concentration. The specific throughput is defined as the volume supplied to the adsorbent divided by the mass of GAC in the adsorbent until a breakthrough occurs (i.e., Qt_{bk}/M_{GAC}) where M_{GAC} represents the mass of GAC and t_{bk} entails the breakthrough time. The specific throughput is used to quantify the performance of a GAC adsorbent. If the effluent concentration is sufficiently lower than the influent concentration, the specific throughput can be approximated as q_c/C_{inf}, where q_c is an averaged adsorbate concentration in the equilibrated GAC column.

Table 1 summarizes studies that examined the effects of soil type on the performance of various LID/BMP in terms of the organic and inorganic removal. The results of these studies cannot be cross-compared as they measured different performance indicators. Among them, Xiao and McPherson performed field experiments and observed the performance of engineered soil and trees in a bioswale built next to a parking lot [88]. During the testing period from February 2007 to October 2008, a total precipitation of 563.8 mm was reported by 50 storm events. The bioswale had a length of 10.4 m, a width of 2.4 m, and depth of 0.9 m. The engineered soil media, composed of a mixture of 75% lava rock and 25% loam fractions, had a total volume

Table 1
Studies that examined granular adsorption by LID/BMP

LID type	Soil	Pollutant	Removal (%)	Scale
Bioretention [5]	Sand, soil, and mulch	P	67.0–98.0%	Laboratory
Bioswale [88]	Engineered Soil (75% lava rock and 25% loam soil)	Minerals	95.3%	field
		Metals	86.7%	
		Organic carbon	95.5%	
		Solids	95.5%	
Rain Garden [89]	Sand	Cu	56.4–93.3%	Laboratory
		Pb	81.6–97.3%	
		Zn	73.5–94.5%	
	Sand/topsoil	Cu	53.0–77.4%	
		Pb	89.1–96.9%	
		Zn	81.2–87.9%	
	Topsoil	Cu	00.3–69.0%	
		Pb	89.5–98.6%	
		Zn	60.5–71.4%	
General LID [90]	Biochar	Metals/metalloids	0.00–75.0%	Laboratory and field (review)
		Organic contaminants	45.0–100%	
		Nutrients	29.2–100%	
Bioretention [91]	Sand/compost, sand, pea stone, and gravel layers without sorbtive media	TSS	89.0–97.0%	Laboratory and field
		N	38.0–57.0%	
		P	86.0–94.0%	

of 28.3 cubic meters and was surrounded by a fine graded non-woven geotextile. A pollutant removal study was conducted for minerals, metals, organic carbon, and solids, as shown in Table 1. Their average pollutant loading reduction was reported as 95.4%; this is in addition to the 86% iron removal and 97% nitrogen removal. As these solutes are directly from stormwater runoff, their specific chemical forms were not reported. Hsieh et al. studied phosphorus removal from urban stormwater runoff using repetitive (lab-scale) bioretention columns. In their study, two types of columns are used called RP1 and RP2 [5]. They examined dual-layer RP1/RP2 configuration where the media of low/high hydraulic conductivity are overlapped with high/low hydraulic conductivity. The column having the length of 40 cm and the inner diameter of 6.4 cm was designed to have sufficient organic matter to serve as a plant growth media. During the three months of experiments, they concluded that RP2, consisting of more conventional media, is more efficient in total removal of phosphorus, dissolved from sodium phosphate dibasic (Na_2HPO_4). The input phosphorous concentration is 3 mg/L and the effluent concentration varies from 0.55 to 1.2 mg/L, which is equivalent to the total phosphorus removal ratio shown in Table 1. Good et al. built lab-scale rain garden systems for stormwater treatment, consisting of topsoil-only, topsoil/sand mixture, and sand-only compositions [89]. The rain garden is of mesocosm-scale having a cylindrical configuration with 180 L internal volume and 0.17 m^2 surface area. The thickness of the top mulch layer above the topsoil was 20 mm in order to mimic the diffusive motion of stormwater across the column of the vegetation layer. An organic topsoil was investigated for the removal of heavy metals (such as Zn, Cu, and Pb) and nitrate. The well-graded coarse sand layer was prepared to provide hydraulic throughput under given rain events. Based on their experimental data shown in Table 1, they concluded that the topsoil is not the optimal substrate to enhance metal or nutrient removal in bioinfiltrative systems, which can be attributed to the inability of topsoil to buffer the pH of incoming stormwater. Mohanty et al. discussed biochar, a carbonaceous porous adsorbent, application as a soil media in general LID systems for stormwater treatment [90]. The pollutant removal and runoff reduction by biochar are determined by various factors, such as particle size, roughness, porosity, hydrophobic surfaces, redox active sites, ash/mineral content, surface function groups, and biological activities. Shrestha et al. studied nutrient and sediment removal in roadside bioretention systems using various soil media, vegetation, and hydrologic treatments [91]. A total of 121 storms were evaluated for the removal of total suspended solids, nitrate/nitrite-nitrogen, ortho-phosphorus, total nitrogen, and total phosphorus. Ranges of removal efficiencies of total suspended solids, total nitrogen, and total phosphorus are summarized in Table 1. Negative removal values were often listed in their work, which must be attributed to the adsorbed fractions of solutes from the previous storm events. Due to the high organic nitrogen portion, the aerobic condition is required in the soil media to drive mineralization consisting of ammonification and nitrification. On the other hand, the phosphorus removal is deteriorated due to the saturation of the soil media due to the desorption of soluble phosphorus. They concluded that the nitrogen removal is closely linked to the microbial processes (i.e., nitrification and denitrification), but phosphorus removal heavily relies on soil chemical parameters of

the timescale. Although Table 1 implies that a LID type can be classified by it's nutrient removal characteristics, representative LID structures such as bioretention, bioswale, and rain garden are originally classified by their geometrical and hydrological aspects. (See the next section for details.) Charlesworth et al. analyzed the application of green and food-based compost to enhance water quality in SUDS/LID devices including swales [92]. They observed that both green compost (GC) and food/green-mixed compost (MC) demonstrated improved performance compared to topsoil in pollutant removal; however, pollutant removal efficiencies were not specifically reported. Trowsdale and Simcock monitored the performance of bioretention consisting of topsoil, subsoil, and sand layers [93] and observed high removal efficiencies of TSS, Pb, and Zn due to the heterogeneous profile of soil permeabilities. The measured data set was only partially reported. Davis et al. summarized the current knowledge on the removal capability of bioretention units for suspended solids, nutrients, hydrocarbons, and heavy metals using, in principle, filtration, adsorption and possibly biological treatment. They indicated the necessity of systematic research on composition and configuration of filling media, drainage configuration, basin geometry, ponding depth, vegetation types, and cost analysis for maintenance and various designs [94]. Moreover, Hunt et al. considered a bioretention as one of the most commonly used stormwater control measures (SCMs) and researched on how to design the bioretention systems to meet regulatory needs. Specific guidelines were reviewed for geometric sub-zones (called components), fluid dynamic (peak-flow mitigation, hydrology and infiltration), chemical (sequestration of total dissolved solid, pathogen-indicator species, metals and hydrocarbon, phosphorous removal, and thermal pollutant abatement) and biological (nitrogen removal) aspects [95]. It is difficult to make a quantitative conclusion for bioswales' removal capabilities of various solute species due to the lack of fundamental theories and systematically prepared data sets.

2.7. Underground drainage

If the bioswale soil is partially saturated or unsaturated, the infiltration of incompressible water into the porous soils pushes pre-existing (compressible) air in the interstitial void spaces between soil grains. Therefore, the surface flow above the bioswale does not move uniformly so as to quickly reach a steady state. This fluid behavior may be a result of micro-scale heterogeneity of the soil packing and the air compressibility. On the other hand, installation of the drainpipe is an optional commitment. Perforated pipe systems can be employed to improve water drainage, reduce sub-grade moisture, and convey stormwater offsite promptly. These drainpipes are extensively applied in various LID/BMP strategies including bioretention ponds [96], bioswales [37], exfiltration trenches [97], French drains [98], infiltration trenches [99], permeable pavements [100], and rain gardens [101]. Table 2 shows the original definitions or descriptions of three LID structures, i.e., bioretention [94], rain gardens [102], and bioswales [103] in terms of geometrical and hydrologic aspects. This is because, in our opinion, pollutant transport and removal processes are not significantly influenced by the LID dimensions and structures. Standard pipe materials include corrugated steel, corrugated aluminum, and polyvinyl chloride. Small holes or slits are periodically formed along the drainpipe. The mean distance between two consecutive holes ranges from 3 to 6 inches [104]. These holes are usually downward facing in order to prevent gravitational clogging. The collected water in the drainpipe is conveyed to the discharging system or to the natural environment.

The hydraulic behavior of perforated pipes has been examined since the early 20th century [104,105]. The pipe geometry is often complex, and, therefore, analytic solutions for the fluid flow are challenging to obtain. Instead, fundamental CFD modeling can provide accurate solutions for coupled mass, momentum, and heat transfer, in principle, but it often requires high-performance computing. To the best of our knowledge, CFD tools have been employed only in the past decade to understand the discharge characteristics of the perforated pipes for LID and BMP [25]. As state above, Afrin et al.'s work focused on the flow patterns and streamlines porous bioswales [25], and the perforated void portion of the pipe surface is exploited as an exit boundary. Their 3D model was validated using experimental results of fluid flows but did not include overland and infiltrating flows on the topsoil of the bioswale. The infiltration direction is usually oblique in the unsaturated aggregate zone but remained in their study primarily vertical in the saturated soil zone. This result implies that considering a porous pipe

Table 2
Original definitions of key LID structures

LID/BMP Device	Definition
Bioretention [94]	"General features of a bioretention system include 0.7–1.0 m of sand/soil/organic media for treating infiltrating storm-water runoff, a surface mulch layer, various forms of vegetation, orientation to allow 15–30 cm of runoff pooling and associated appurtenances for inlet, outlet, and overflow."
Rain garden [102]	"Rain gardens are shallow depressions in the landscape that are planted with trees and/or shrubs, and covered with a bark mulch layer or ground cover. They allow stormwater to infiltrate, recharge aquifers, and reduce peak flows. In addition, they are expected to provide pollutant treatment, which has been attributed to several processes including adsorption, decomposition, ion exchange, and volatilization."
Bioswales [103]	"Bioswales are generally at least 30 m (100 ft) long, 0.6 m (2 ft) wide, range in longitudinal slope from 0.5% to 6.0%, and located in series with detention ponds, which store runoff and reduce peak discharges. Although they are designed to convey runoff from the 100-year 24-h storm event, they are only intended to treat runoff effectively from much smaller and more frequent storms, typically up to the 2-year 24-h storm event."

as an orifice is not a valid assumption for the momentum transport in bioswale systems. Infiltrating water occupies the void space in the unsaturated zone and consequently pushes air blobs downward. Buoyant forces offer balance to the hydrodynamic drag on the air blobs. Therefore, the channeling of air occurs in the dynamic saturated zone during the process of infiltration, which is due to the local heterogeneity of micro-packing structure soil grains and the initial distribution of the blobs. This exchanging phenomena of water and air fluids in the porous bioswale is currently not found in the related literature and will be studied in our next CFD paper.

The types of drain pipe structures employed in bioswale systems can be classified into three categories: no drain, a linear drain, and elevated drain. The drainpipe is not a mandatory element of a bioswale, but it may determine the available amounts of drainage and retention of a bioswale. After an exhaustive saturation of the bioswale due to precipitation events, evapotranspiration can form the only physical mechanism to remove the infiltrated water inside the soil grain surfaces. Unless biological degradation is consistent, convected pollutants may continuously accumulate on soil grain surfaces depending on the adsorption capability of the engineered soil. Consequently, the capacities of granular media and activated carbon will reach their maximum limits. The long-term accumulation of organic/inorganic/particulate pollutants in bioswales can cause further leaching problems which cause unscheduled replacements of soil matrixes. Disposal of the contaminated soil grains generates another challenge within the bioswale maintenance. In our opinion, the optimal usage of the bioswale should include a periodic dilution of the pollutant level by artificially flushing the bioswale using low-cost water [105–110].

A linear drain installation includes a typical cylindrical pipe with periodic perforation, installed horizontally near the bottom of the bioswale. Neighboring zones around the linear pipe are often prepared using coarse grains to allow the fast discharge of infiltrated water and, more importantly, to prevent pipe clogging due to fine grains. The drainpipe is usually installed in the longitudinal direction of a bioswale, but the main pipe can be connected to transverse pipes for faster discharge appearing at regular intervals. This transverse configuration treats a long bioswale as a series of small independent bioswale units, which give evenly distributed draining performance. The transverse pipe outlet can be elevated to maintain a specific depth of saturated zone above the drainpipe. Consequently, this configuration prevents soil compaction and pipe clogging, which are caused by the complete dryness of the soil layer. The elevated pipe configuration requires the periodic dilution process to maintain a low pollutant level inside the bioswale. More significantly, microbial activities can be maintained in the semi-permanently/permanently saturated zone, depending on flow patterns in the subsurface. Chemical equilibrium can be attained for a short span of time immediately after the end of a storm event. Residual pollutant concentration from the previous storm event may primarily contribute to the discharge concentration of the subsequent storm event [81,111]. The drainpipe not only discharges infiltrate water but also controls hydrodynamic and chemical reactions in the bioswale. For example, one can often observe mass-balance violation due to the initial conditions of a bioswale. If infiltration of the last storm event (of high runoff pollutant concentration) ended at the final stage of the storm, the residual pollutants must remain within the bioswale in either the dissolved or absorbed phase. If the next rain event contains low runoff concentrations, then the first effluent from the bioswale must have a (much) higher concentration than that of the new influent. The prediction of the first influent concentration requires very detailed local information within the soil zone of the bioswale, which seems to be challenging.

3. CFD as a universal modeling platform

Sustainable and renewable strategies can strategically mitigate stormwater threats, but present-day design methodologies emphasize only minimal, required criteria [112,113]. More specific and reliable design tools are, therefore, urgently needed for optimized LID/BMP practices. In our opinion, LID/BMP structures without regional optimizations can cause unexpected hydrologic events unless the plane runoff patterns are holistically well-understood. In this light, we propose CFD as a universal modeling tool for design and optimization of LID/BMP systems [114,115]. In this section we discuss the future direction of bioswale CFD modeling so as to systematically elucidate upon the coupled transport phenomena.

Within most engineering processes, a fluid flow often provides a platform for mass and heat transfer. For complex systems, interfaces and boundaries play critical roles in transferring physical quantities from one phase to the other. Dominant transport phenomena of a bioswale can be considered within various sub-zones as follows. First, on the topsoil surface of the bioswale, the entering overland flow is separated into infiltration and discharge, and flow pattern within the vegetated layer depends on the overall plant configuration. Therefore, the coupling of the open-channel and porous-media flows should be carefully merged for the topsoil boundary surface of the bioswale. Second, the infiltration within the vegetation layer enhances the sedimentation of suspended solids, which initiates the surface clogging. The hydrodynamic resistance will gradually increase and reduce the infiltration rate. The feedback effect of cake layer formation caused by deposited particles should be included in the long-term simulation of the bioswale performance while a constant thickness of the clogging layer can be assumed for short-term studies. Third, the infiltrating flow carries fine particles, a fraction of which will be filtered by soil grains. A phenomenon similar to the standard GMF occurs in the bulk phase of the porous bioswale. A unique difference between the bioswale system and conventional GMF for particle filtering is the heterogeneous, unsteady distribution of unsaturated zones and the dynamic migration of the zone boundary. Fundamental mechanisms regarding the particle transport near the zone boundary continues to be an area of active research. Fourth, organic and inorganic reactions primarily depend on concentrations of solute species in the infiltrated runoff water because the timescale for the chemical equilibrium is much shorter than the respective particle relaxation time. The solute species can be assumed to be in equilibrium to those

adsorbed on the soil grain surfaces. In this case, the interstitial flow brings solutes to the vicinity of the soil grains but does not noticeably affect the pollutant removal efficiency due to the instantaneously reached equilibrium state. The validity of this local equilibrium approach depends on the grain size distribution, which mainly determines the hydraulic conductivity or permeability. Finally, the interstitial flow reaches the drainpipe and exits the porous media into an open space, such as a receiving water body. This exit water-flow is balanced by the reversely entering airflow from the drainpipe to the porous region near the pipe. This volume exchanging phenomenon between water and air flows is also significant during the initial infiltration stage. To the best of our knowledge, this phase-exchange phenomena has not been reported in the bioswale literature and will be addressed in our next research.

Overall, the transport phenomena of the bioswale can be summarized as the changes of flow regimes from free space to the porous media and from the porous media to the drainpipe. The dominant factors that alter the interstitial flow pattern include the heterogeneity of soil structures followed by the initial distribution of air blobs in the unsaturated bioswale. Assuming solutes are not volatile, physical and chemical removal of suspended particles and chemical species depends upon the local infiltration patterns. In this case, the mass transport mechanisms, such as convection, diffusion, and reaction, can be treated as perturbative transport phenomena occurring on top of ambient, interstitial fluid flows. The mass removal processes do not provide noticeable feedback effects to fluid flows. Treating the soil grain packings as a continuous, homogeneous porous media, two-phase CFD can accurately predict the flow of water and air. The mass transport phenomena can be independently studied using the simulation results of fluid motion afterward. Based on our current review, we observed that the flow coupling at the topsoil surface is the most critical sub-process that determines the bioswale performance. Analytic solutions for the two-phase flow having multiple interfaces is theoretically a difficult task. CFD simulations with specific solute transport mechanism can therefore give more fundamental and accurate prediction of the bioswale performance.

4. Concluding remarks

In this study, we reviewed dominant transport mechanisms inside the bioretention system by treating a bioswale as a miniature water and wastewater treatment plant. Fluid dynamic aspects consist of runoff, overland, infiltration and discharge flows. The mass transfer phenomena reviewed include sedimentation of suspended particles, conventional filtration of fine particles, and removal of organic and inorganic pollutants because unsteady variations of (micro) biological processes are theoretically challenging and more importantly chemical, physical and fluid dynamic conditions provide basic conditions to the biological process. We restrict ourselves to physical, chemical, and fluidic processes, excluding biological reactions. Within each subtopic of fluid dynamic and mass transfer phenomena, key theories were selected and examined in detail to construct a universal model as a seamless combination of well-defined unit processes. Due to the intrinsic challenges involved with data acquisition, the current bioswale research is limited to empirical studies and data fitting based on simple flow models or mass balance equations. CFD is proposed as a universal modeling platform in the application of bioswale research because it can predict various mass transfer mechanisms as passive transport phenomena in the pre-determined, multi-zone flow fields. The size of LID/BMP systems is significant because these devices are almost permanently installed. Considerably more work will be needed to include detailed optimization tests using CFD for various hydrologic and physico-chemical scenarios, which will be discussed in our future publications.

Acknowledgments

This work was supported by the Kohala Center of Hawaiian Scholars Doctoral Fellowship Program (formerly known as the Mellon-Hawai‘i Doctoral and Postdoctoral Fellowship Program), the Deviants from the Norm Fund and Dr. Paul and Elizabeth Nakayama for the first author. The authors appreciate Mr. Curtis Matsuda at the Hawaii Department of Transportation for his inspiring discussions.

References

[1] National Research Council, A report of the national research council: Urban stormwater management in the United States, The National Academies Press, Washington D.C., 2008.
[2] National Research Council, Urban Stormwater Management in the United States, The National Academies Press, Washington D.C., 2009.
[3] US EPA, Storm Water Technology Fact Sheet - wet detention ponds. Fact sheet, 1999.
[4] Prince George's County, Stormwater Management Design Manual, 2014.
[5] C. Hsieh, A.P. Davis, B.A. Needelman, Bioretention column studies of phosphorus removal from urban stormwater runoff, Water Environ. Res., 790 (2007) 177–184.
[6] P. Hamel, T.D. Fletcher, The impact of stormwater source-control strategies on the (low) flow regime of urban catchments, Wat. Sci. Technol., 690 (2014) 739–745.
[7] C. Yu, J. Duan, Simulation of surface runoff using hydrodynamic model, J. Hydrol. Eng., 6 (2017) 1–12.
[8] A. Roy-Poirier, Y. Filion, P. Champagne, An event-based hydrologic simulation model for bioretention systems, Water Sci. Technol., 720 (2015) 1524–1533.
[9] R.A. Brown, R.W. Skaggs, W.F. Hunt, Calibration and validation of DRAINMOD to model bioretention hydrology, J. Hydrology, 486 (2013) 430–442.
[10] J. Yazdi, S.A.A. Salehi Neyshabouri, Environmental modelling & software identifying low impact development strategies for flood mitigation using a fuzzy-probabilistic approach, Environ. Model. Software, 60 (2014) 31–44.
[11] A.B. Barton, J.R. Argue, Integrated urban water management for residential areas: A reuse model, Wat. Sci. Technol., 600 (2009) 813–823.
[12] L. Ahiablame, R. Shakya, Modeling flood reduction effects of low impact development at a watershed scale, J. Environ. Manage., 171 (2016) 81–91.
[13] J. Gwang, A. Selvakumar, K. Alvi, J. Riverson, J.X. Zhen, L. Shoemaker, F. Lai, Environmental modelling and software a watershed-scale design optimization model for stormwater best management practices, Environ. Model. Software, 60 (2012) 6–18.

[14] J. Gao, R. Wang, J. Huang, M. Liu, Application of BMP to urban runoff control using SUSTAIN model: Case study in an industrial area, Ecol. Model., 318 (2015) 177–183.
[15] R.A. Brown, R.W. Skaggs, W.F. Hunt III, Calibration and validation of DRAINMOD to model bioretention hydrology, J. Hydrology, 486 (2013) 430–442.
[16] A. Palla, I. Gnecco, Hydrologic modeling of low impact development systems at the urban catchment scale, J. Hydrology, 528 (2015) 361–368.
[17] P. Xu, F. Gao, J. He, X. Ren, W. Xi, Modelling and optimization of land use/land cover change in a developing urban catchment, Wat. Sci. Technol., 75 (2017) 2527–2537.
[18] A.A. Bloorchian, L. Ahiablame, A. Osouli, J. Zhou, Modeling BMP and vegetative cover performance for highway stormwater runoff reduction, Procedia Eng., 145 (2016) 274–280.
[19] I.M. Brodie, Prediction of stormwater particle loads from impervious urban surfaces based on a rainfall detachment index, Wat. Sci. Technol., 51 (1999) 49–56.
[20] J. Zimmermann, C. Dierkes, P. Göbel, C. Klinger, H. Stubbe, W.G. Coldewey, Metal concentrations in soil and seepage water due to infiltration of roof runoff by long term numerical modelling, Wat. Sci. Technol., 51 (2005) 11–19.
[21] I.M. Brodie, SSUIS - A research model for predicting suspended solids loads in stormwater runoff from urban impervious surfaces, Wat. Sci. Technol., 65 (2012) 2140–2147.
[22] J.M. Hathaway, R.A. Brown, J.S. Fu, W.F. Hunt, Bioretention function under climate change scenarios in North Carolina, J. Hydrology, 519 (2014) 503–511.
[23] V. Stovin, S. Poë, C. Berretta. A modelling study of long term green roof retention performance, J. Environ. Manage., 131 (2013) 206–215.
[24] Y. Li, R.W. Babcock, Green roof hydrologic performance and modeling: A review, Wat. Sci. Technol., 69 (2014) 727–738.
[25] T. Afrin, A.A. Khan, N.B. Kaye, F.Y. Testik, Numerical model for the hydraulic performance of perforated pipe underdrains surrounded by loose aggregate numerical model for the hydraulic performance of perforated pipe underdrains surrounded by loose aggregate, J. Hydraul. Eng., 145 (2016) 1–10.
[26] C. Hsieh, A.P. Davis, Evaluation and optimization of bioretention media for treatment of urban storm water runoff, J. Environ. Eng., 131 (2005) 1521–1531.
[27] A. Roy-poirier, P. Champagne, A.M. Asce, Y. Filion, Review of bioretention system research and design: past, present, and future, J. Environ. Eng., (2010) 878–889.
[28] F.E. Botros, Y.S. Onsoy, T.R. Ginn, T. Harter, Richards equation based modeling to estimate flow and nitrate transport in a deep alluvial vadose zone, Vadose Zone J., (2012) 1–16.
[29] W.H. Green, G.A. Ampt, Studies on Soil Physics, Part I. The flow of air and water through soils, J. Agric. Sci., 4 (1911) 1–24.
[30] R.G. Mein, C.L. Larson, Modeling the infiltration component of the rainfall-runoff process, Water Resources Research Center, University of Minnesota, Technical report, 1971.
[31] R.G. Mein, C.L. Larson, Modeling infiltration during a steady rain, Wat. Resour. Res., (1973) 384–394.
[32] J.Y. Parlange, I. Lisle, R.D. Braddock, R.E. Smith, The three-parameter infiltration equation, Soil Sci., (1982) 337–341.
[33] W.F. Noh, P. Woodward, SLIC (Simple Line Interface Calculation). In Adriaan I van de Vooren and Pieter J Zandbergen, editors, Proceedings of the Fifth International Conference on Numerical Methods in Fluid Dynamics June 28–July 2, 1976 Twente University, Enschede, (1976), 330–340.
[34] C.W. Hirt, B.D. Nichols, Volume of fluid (VOF) method for the dynamics of free boundaries, J. Comp. Phys., 390 (1981) 201–225.
[35] M. García-Serrana, J.S. Gulliver, J.L. Nieber, Non-uniform overland flow-infiltration model for roadside swales, J. Hydrol., 552 (2017) 586–599.
[36] C. McShane, Transforming the use of urban sapce: a look at the revolution in street pavements, 1880–1924, J. Urban History, 5 (1979) 279–307.
[37] US EPA. National Management Measures to Control Nonpoint Source Pollution from Urban Areas, Technical report, 2005.
[38] US EPA. Urban Runoff: Low Impact Development. Polluted Runoff: Nonpoint Source Pollution, Online Factsheet, 2016.
[39] US EPA. National Water Quality Inventory: Report to Congress, Technical report, 2017.
[40] A. Vargas-Luna, A. Crosato, W.S.J. Uijttewaal, Effects of vegetation on flow and sediment transport: Comparative analyses and validation of predicting models, Earth Surface Process, Landforms, 400 (2015) 157–176.
[41] J. Zhang, Y. Zhong, W. Huai, Transverse distribution of streamwise velocity in open-channel flow with artificial emergent vegetation, Ecol. Eng., 110 (2018) 78–86.
[42] K. Shiono, D.W. Knight, Turbulent open-channel flows with variable depth across the channel, J. Fluid Mech., 222 (1991) 617–646.
[43] C. Liu, X. Luo, X. Liu, K. Yang, Modeling depth-averaged velocity and bed shear stress in compound channels with emergent and submerged vegetation, Adv. Wat. Resour., 60 (2013) 148–159.
[44] H.S. Kim, M. Nabi, I. Kimura, Y. Shimizu, Computational modeling of flow and morphodynamics through rigid-emergent vegetation, Adv. Water Resour., 84 (2015) 64–86.
[45] M. Nabi, H.J. De Vriend, E. Mosselman, C.J. Sloff, Y. Shimizu, Detailed simulation of morphodynamics: 1. Hydrodynamic model, Wat. Res., 480 (2012) 1–19.
[46] J. Smagorinsky, General circulation experiments with the primitive equations, Monthly Weather Rev., 910 (1963) 99–164.
[47] M. Gao, W. Huai, Y. Xiao, Z. Yang, B. Ji, Large eddy simulation of a vertical buoyant jet in a vegetated channel, Int. J. Heat Fluid Flow, 700 (2018) 114–124.
[48] J. Lu, H.C. Dai, Three-dimensional numerical modeling of flows and scalar transport in a vegetated channel, J. Hydro-Environ. Res., 16 (2017) 27–33.
[49] W.J. Wang, W.X. Huai, S. Thompson, W.Q. Peng, G.G. Katul, Drag coefficient estimation using flume experiments in shallow non-uniform water flow within emergent vegetation during rainfall, Ecol. Indic., 92 (2018) 367–378.
[50] M.M. Larmaei, T.F. Mahdi, Depth-averaged turbulent heat and fluid flow in a vegetated porous medium, Int. J. Heat Mass Transfer, 550 (2012) 848–863.
[51] N.R. Siriwardene, A. Deletic, T.D Fletcher, Clogging of stormwater infiltration systems and filters: insights from a laboratory study, Wat. Res., 41 (2007) 1433–1440.
[52] S. Achleitner, C. Engelhard, U. Stegner, W. Rauch, Local infiltration devices at parking sites: Experimental assessment of temporal changes in hydraulic and contaminant removal capacity, Wat. Sci. Technol., 550 (2007) 193–200.
[53] Montgomery County Maryland Department of Environmental Protection, How to Maintain Your Rain Barden, Bioswale, and Micro-bioretention Practice, Stormwater Facility Maintenance Program, Technical report, 2013.
[54] G.T. Blecken, W.F. Hunt III, A.M. Al-Rubaei, M. Viklander, W.G. Lord, Stormwater control measure (SCM) maintenance considerations to ensure designed functionality, Urban Wat. J., 14 (2017) 278–290.
[55] D. Jurries, Biofilters (Bioswales, Vegetative Buffers, and Constructed Wetlands) for Storm Water Discharge Pollution Removal, Department of Environmental Quality, State of Oregon, Technical report, 2003.
[56] Washington State Department of Transportation, Vegetative Filter Strips Tutorial, Technical report, 2008.
[57] Iowa Department of Natural Resources, Iowa Stormwater Management Manual, 2013.
[58] E.M. LaBolle, G.E. Fogg, A.F.B. Tompson, Random-walk simulation of transport in heterogeneous porous media: Local mass-conservation problem and implementation methods, Wat. Resour. Res., 320 (1996) 583–593.
[59] M. Bergman, M.R. Hedegaard, M.F. Petersen, P. Binning, O. Mark, P.S. Mikkelsen, Evaluation of two stormwater infiltration trenches in central Copenhagen after 15 years of operation, Wat. Sci. Technol., 630 (2011) 2279–2286.
[60] E. Warnaars, A.V. Larsen, P. Jacobsen, P.S. Mikkelsen, Hydrological behavior of stormwater infiltration trenches in a central urban area during 2 3/4 years of operation, Wat. Sci. Technol., 39 (1999) 217–224.

[61] A.V. Mikkelsen, P.S. Warnaars, E. Larsen, NedsivningAfRegnvand Fra enBoligkarréPåNørrebro, University of Denmark, Technical report, 1999.
[62] S. Le Coustumer, T.D. Fletcher, A.Deletic, S. Barraud, P. Poelsma, The influence of design parameters on clogging of stormwater biofilters: A large-scale column study, Wat. Res., 460 (2012) 6743–6752.
[63] US EPA, Storm Water Management Model User's Manual Version 5.1 Storm Water Management Model, , Cincinnati, Ohio, Technical report, 2015
[64] M.A. Kachchu Mohamed, T. Lucke, F. Boogaard, Preliminary investigation into the pollution reduction performance of swales used in a stormwater treatment train, Wat. Sci. Technol., 690 (2014) 1014–1020.
[65] X. Sun, A.P. Davis, Heavy metal fates in laboratory bioretention systems, Chemosphere, 660 (2007) 1601–1609.
[66] M. Razzaghmanesh, M. Borst, Investigation clogging dynamic of permeable pavement systems using embedded sensors, J. Hydrol., 557 (2018) 887–896.
[67] C. Ulrich, S.S. Hubbard, J. Florsheim, D. Rosenberry, S. Borglin, M. Trotta, D. Seymour, Riverbed clogging associated with a California riverbank filtration system: An assessment of mechanisms and monitoring approaches, J. Hydrol., 529 (2015) 1740–1753.
[68] T. Grischek, R. Bartak, Riverbed clogging and sustainability of riverbank filtration, Water, 80 (2016) 1–12.
[69] L. Locatelli, O. Mark, P.S. Mikkelsen, K. Arnbjerg-Nielsen, T. Wong, P.J. Binning, Determining the extent of groundwater interference on the performance of infiltration trenches, J. Hydrol., 529 (2015) 1360–1372.
[70] K. Yao, M.T. Habibian, C.R. O'Melia, Water and waste water filtration: Concepts and applications, Environ. Eng. Sci., 50 (1971) 1105–1112.
[71] R. Rajagopalan, C. Tien, Trajectory analysis of deep-bed filtration with the sphere-in-cell porous media model, AIChE J., 220 (1976) 523–533.
[72] N. Tufenkji, M. Elimelech, Correlation equation for predicting single-collector efficiency in physicochemical filtration in saturated porous media, Environ. Eng. Sci., 38 (2004) 529–536.
[73] K.E. Nelson, T.R. Ginn, Colloid filtration theory and the Happel sphere-in-cell model revisited with direct numerical simulation of colloids, Langmuir, 210 (2005) 2173–2184.
[74] J. Happel, Viscous flow in multiparticle systems: slow motion of fluids relative to beds of spherical particles, AIChE J., 40 (1958) 197–201.
[75] A.S. Kim, Cylindrical cell model for direct contact membrane distillation (DCMD) of densely packed hollow fibers, J. Membr. Sci., 455 (2014) 168–186.
[76] A.S. Kim, A.E. Contreras, Q. Li, R. Yuan, Fundamental mechanisms of three-component combined fouling with experimental verification, Langmuir, 25 (2009) 7815–7827.
[77] A.S. Kim, R. Yan, Cake resistance of aggregates formed in the diffusion-limited-cluster-aggregation (DLCA) regime, J. Membr. Sci., 286 (2006) 260–268.
[78] A.S. Kim, H. Chen, R. Yuan, EPS biofouling in membrane filtration: an analytic modeling study, J. Colloid Interface Sci., (2006) 243–249.
[79] A.S. Kim, R. Yuan, Hydrodynamics of an ideal aggregate with quadratically increasing permeability, J. Colloid Interface Sci., 285 (2005) 627–633.
[80] A.S. Kim, R. Yuan, A new model for calculating specific resistance of aggregated colloidal cake layers in membrane filtration processes, J. Colloid Interface Sci., 249 (2005) 89–101.
[81] J.J. Lenhart, J.E. Saiers, Transport of silica colloids through unsaturated porous media: Experimental results and model comparisons, Environ. Sci. Technol., 360 (2002) 769–777.
[82] W. Zhang, V.L. Morales, M.E. Cakmak, A.E. Salvucci, L.D. Geohring, A.G. Hay, J. Parlange, T.S. Steenhuis, Colloid transport and retention in unsaturated porous media: Effect of colloid input concentration, Environ. Sci. Technol., 440 (2010) 4965–4972.
[83] T. Knappenberger, M. Flury, E.D. Mattson, J.B. Harsh, Does water content or flow rate control colloid transport in unsaturated porous media? Environ. Sci. Technol., 480 (2014) 3791–3799.
[84] S. Xu, J. Qi, X. Chen, V. Lazouskaya, J. Zhuang, Y. Jin, Coupled effect of extended DLVO and capillary interactions on the retention and transport of colloids through unsaturated porous media, Sci. Total Environ., 573 (2016) 564–572.
[85] J.W. Delleur, New results and research needs on sediment movement in urban drainage, J. Wat. Res. Planning Manage., 1270 (2001) 186–193.
[86] I. Langmuir, The adsorption of gases on plane surfaces of glass, mica and platinum, J. Am. Chem. Soc., 400 (1918) 1361–1403.
[87] H. Freundlich, Über die adsorption in lösungen. ZeitschriftfürPhysikalische, Chemie, 57 (1906) 385–470.
[88] Q. Xiao, E.G. McPherson, Performance of engineered soil and trees in a parking lot bioswale, Urban Wat. J., 80 (2011) 241–253.
[89] J.F. Good, A.D. O'Sullivan, D. Wicke, T.A. Cochrane, Contaminant removal and hydraulic conductivity of laboratory rain garden systems for stormwater treatment, Wat. Sci. Technol., 650 (2012) 2154–2161.
[90] S.K. Mohanty, R. Valenca, A.W. Berger, I.K.M. Yu, X. Xiong, T.M. Saunders, D.C.W. Tsang, Plenty of room for carbon on the ground: Potential applications of biochar for stormwater treatment, Sci. Total Environ., 625 (2018) 1644–1658.
[91] P. Shrestha, S.E. Hurley, B.C. Wemple, Effects of different soil media, vegetation, and hydrologic treatments on nutrient and sediment removal in roadside bioretention systems, Ecol. Eng., 1120 (2018) 116–131.
[92] S.M. Charlesworth, E. Nnadi, O. Oyelola, J. Bennett, F. Warwick, R. Jackson, D. Lawson, Laboratory based experiments to assess the use of green and food-based compost to improve water quality in a sustainable drainage (SUDS) device such as a swale, Sci. Total Environ., 424 (2012) 337–343.
[93] S.A. Trowsdale, R. Simcock, Urban stormwater treatment using bioretention, J. Hydrol., 3970 (2011) 167–174.
[94] A.P. Davis, W.F. Hunt, R.G. Traver, M. Clar, Bioretention technology: overview of current practice and future needs, J. Environ. Eng., 135 (2009) 109–117.
[95] W.F. Hunt, A.P. Davis, R.G. Traver, Meeting hydrologic and water quality goals through targeted bioretention design, J. Environ. Eng., 138 (2012) 697–707.
[96] Water by Design, Bioretention Technical Design Guidelines, Technical report, Healthy Water Waterways Ltd, Brisbane, 2014.
[97] D.A. Chin, An Overview of Urban Stormwater Management Practices in Miami-Dade County, Florida, Technical report, U.S. Geological Survey, 2004.
[98] NDS, NDS Principles of Exterior Drainage: Short Course, Technical report, Lindsy, CA, 2007
[99] Virginia Department of Environmental Quality, Virginia DEQ Stormwater Design Specification Infiltration Practices, Technical report 8, 2013.
[100] M. Kayhanian, P.T. Weiss, J.S. Gulliver, L. Khazanovich, The Application of Permeable Pavement with Emphasis on Successful Design, Water Quality Benefits, and Identification of Knowledge and Data Gaps: A Summary Report, National Center for Sustainable Transportation, Technical report, 2015.
[101] F. Jaber, D. Woodson, C. LaChance, Y. Charriss, Stormwater Management: Rain gardens, Texas A&M AgriLife Extention, Technical report, 2012.
[102] M.E. Dietz, J.C. Clausen. A field evaluation of rain garden flow and pollutant treatment, Water Air, Soil Poll., 167 (2005) 123–138.
[103] G. Mazer, D. Booth, K. Ewing, Limitations to vegetation establishment and growth in biofiltration swales, Ecol. Eng., 17 (2001) 429–443.
[104] North American Pipe Corporation, ASTM F758 PVC Highway Underdrain Pipe Solvent Weld, Technical report, 2017.
[105] H.N. Jenks, An investigation of perforated-pipe filter underdrains, Eng. News-Rec. (1921) 162–166.
[106] US Army Corps of Engineers, Investigation of Filter Requirements for Underdrains, Technical report, 1941.
[107] G. Roinas, C. Mant, J.B. Williams, Fate of hydrocarbon pollutants in source and non-source control sustainable drainage systems, Wat. Sci. Technol., 690 (2014) 703–709.

[108] H. Li, K. Li, X. Zhang, Performance evaluation of grassed swales for stormwater pollution control, Procedia Eng., 154 (2016) 898–910.
[109] J. Li, C. Jiang, T. Lei, Y. Li, Experimental study and simulation of water quality purification of urban surface runoff using non-vegetated bioswales, Ecol. Eng., 95 (2016) 706–713.
[110] Ü. Mander, J. Tournebize, K. Tonderski, J.T.A. Verhoeven, W.J. Mitsch, Planning and establishment principles for constructed wetlands and riparian buffer zones in agricultural catchments, Ecol. Eng., 103 (2017) 296–300.
[111] R.A. Purvis, R.J. Winston, W.F. Hunt, B. Lipscomb, K. Narayanaswamy, A. McDaniel, M.S. Lauffer, S. Libes, Evaluating the water quality benefits of a bioswale in Brunswick County, North Carolina (NC), USA, Water, 100 (2018) 1–16.
[112] P. Gobel, C. Dierkes, W.G. Coldewey, Storm water runoff concentration matrix for urban areas, J. Contaminant Hydrol., 910 (2007) 26–42.
[113] National Oceanic and Atmospheric Administration, Low Impact Development a Practitioner's Guide for Hawaii, Technical report, 2006.[112] City and County of Honolulu, Department of Planning and Permitting, Storm Water BMP Guide for New and Redevelopment, Technical report, 2017.
[114] C. Li, T.D Fletcher, H.P. Duncan, M.J. Burns, Can stormwater control measures restore altered urban flow regimes at the catchment scale? J. Hydrol., 549 (2017) 631–653.
[115] H.E. Golden, N. Hoghooghi, Green infrastructure and its catchment-scale effects: an emerging science. Wiley Interdisciplinary Reviews, Water, (2018) 1–14.